DOI: 10.1002/chem.201000417

Spectroscopic Implications of the Electron Donor–Acceptor Effect in the Photoactive Yellow Protein Chromophore

Tomás Rocha-Rinza,*[a, b] Ove Christiansen,[a] Dennis B. Rahbek,[c] Benedikte Klærke,[c] Lars H. Andersen,[c] Kasper Lincke,[d] and Mogens Brøndsted Nielsen[d]

Abstract: The importance of the donor–acceptor push–pull system in the photoabsorption of the *trans p*-coumaric acid, the cofactor within the photoactive yellow protein and other xanthopsins, has been investigated. We recorded gas-phase absorption spectra and performed high-level quantum chemical calculations of three chromophore models, namely, the deprotonated *trans ortho*-, *meta*- and *para*-methyl coumarates. The *ortho* and *para* isomers, which have the electron-donating phenoxy oxygen and the electron-withdrawing acyl group in conjugation, present absorptions in the high-energy region of the visible spectrum, that is, in the interval of wavelengths in which the photoactivity of the xanthopsins is observed. On the other hand, the *meta* isomer, in which the conjugation between the phenoxy and acyl groups is disrupted, exhibits a significantly shifted maximum and presents no absorption in the region from blue to ultraviolet A. It is found that the push–pull system in the *trans p*-coumaric acid is critical for the wavelength and the intensity of its photoabsorption. Absorption spectra were also measured in methanol and showed an appreciable hypsochromic effect. Linear response calculations within the formalism of the approximate coupled cluster singles and doubles CC2 model and time-dependent DFT using the functional CAM-B3LYP provided insights into the relevant processes of excitation and aided to the interpretation of the experimental results. There is good agreement between theory and experiment in the description of the gas-phase absorption spectra of the considered chromophore models. Differential density plots were used to predict the effect of hydrogen-bonded amino acids to the *trans p*-coumaric acid on the protein tuning of this chromophore.

Keywords: absorption spectra · density functional calculations · donor–acceptor systems · photoactive yellow proteins · xanthopsins

Introduction

The photoactive yellow protein (PYP) is a cytoplasmic protein that was first isolated from *Ectothiorhodospira halophila* (now *Halorhodospira halophila*) and is associated with the blue-light repellent response of its host.[1,2] PYP is the prototype of the family of xanthopsins, which are biological photoreceptors containing a covalently bound, deprotonated *p*-coumaric acid (pCA$^-$) as a light-absorbing chromophore in the dark ground state of the protein.[3] Xanthopsins have been exclusively found in aquatic and anoxygenic photosynthetic *Proteobacteria* and they have been related with diverse output signals, including photomovement and regulation in the expression of the chalcone synthase gene involved in the production of photoprotective pigments.[4,5] Besides its biological role, PYP has become a paradigm in studies of the primary photochemistry of light sensing and functional protein dynamics involved in biological signaling,[6] to such an extent that its importance in this respect is now comparable with the rhodopsins.[7] The attractiveness of

[a] Prof. Dr. T. Rocha-Rinza, Prof. Dr. O. Christiansen
Lundbeck Foundation Center for Theoretical Chemistry and
Center for Oxygen Microscopy (COMI), Department of Chemistry
University of Aarhus, 8000 Aarhus C (Denmark)

[b] Prof. Dr. T. Rocha-Rinza
Present address: Instituto de Química, UNAM, Circuito Exterior
Ciudad Universitaria, Delegación Coyoacán C.P. 04510
Mexico, D.F. (Mexico)
Fax: (+52) 555-616-2217
E-mail: tomasrocharinza@gmail.com

[c] D. B. Rahbek, B. Klærke, Prof. L. H. Andersen
Department of Physics and Astronomy, University of Aarhus
8000 Aarhus C (Denmark)

[d] K. Lincke, Prof. Dr. M. Brøndsted Nielsen
Department of Chemistry, University of Copenhagen
2100 Copenhagen Ø (Denmark)

Supporting information for this article is available on the WWW under http://dx.doi.org/10.1002/chem.201000417.

PYP as a model in photobiology is based on its favorable handling characteristics: it has a low molecular weight and considerable photostability, it is water soluble, and forms crystals from which high-resolution structures are readily available.[1,2] In addition, the photochemical activity of PYP is amenable to be investigated by a wide variety of biophysical techniques.[1,2,6]

The spectral properties of pCA$^-$ are crucial for the photoresponse of PYP and other xanthopsins. Gas-phase absorption spectra are important because they allow the testing of the inherent spectral characteristics of the cofactor of a light-sensing protein in an environment devoid of charges, dipoles, or dielectrics.[8] The gas-phase photoabsorption spectrum of pCA$^-$ presents a maximum at 2.88 eV (430 nm),[9,10] which is just outside the range of absorption maxima of different xanthopsins that span from 2.67 eV (465 nm) to 2.86 eV (434 nm).[13,5] This indicates that the intrinsic absorption of pCA$^-$ within the xanthopsins is not substantially changed, in accordance with the notion that the chromophore inside a photoactive protein must suit the wavelength interval in which the holoprotein needs to be active.[1] In the case of PYP, the absorption of pCA$^-$ in aqueous phase is strongly blueshifted with respect to the gas-phase spectrum: it presents a maximum of absorption at 4.35 eV (285 nm) and a shoulder at 3.97 eV (312 nm).[9] The absence of perturbations from a surrounding medium makes gas-phase absorption spectra a better reference than those obtained in solution for evaluating protein tuning and, importantly, for tests of ab initio calculations.

Electronic delocalization is among the most important issues in the spectral response of chromophores. In this regard, pCA$^-$ can be conceived as a push–pull system, that is, a molecule with an electron-withdrawing group (the acyl, −COX, group) conjugated to an electron-donor moiety (the negatively charged oxygen bond to the benzene ring). This article addresses the importance of the push–pull system in pCA$^-$ by measuring the absorption spectra of the deprotonated *ortho*- (oCMe$^-$), *meta*- (mCMe$^-$) and *para*- (pCMe$^-$) methyl coumarates shown in Scheme 1. The electronic communication between donor and acceptor ends in these three regioisomers differs significantly. In particular, the donor–acceptor coupling in the *meta* isomer should be different from that of the *ortho* and *para* compounds, as suggested from a simple analysis of resonance structures. The employed methyl esters are preferable to their carboxylic acid counterparts because their use prevents the gas-phase prototropic tautomerism between carboxylate and phenoxide isomeric forms, which may be present in pCA$^-$.[10] This ensures the recording of the phenoxide structure present in the ground state of PYP and other xanthopsins. Finally, we also performed ab initio calculations to complement and facilitate the interpretation of our experimental results.

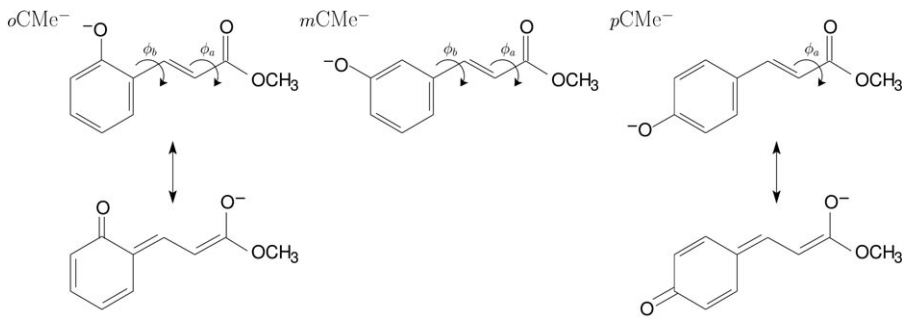

Scheme 1. Structures of the deprotonated methyl coumarates as PYP chromophore models considered in this work. The angles ϕ_a and ϕ_b designate the single-bond rotations addressed to study the consequences of the conformational isomerism on the calculation of vertical excitation energies.

Experimental and Computational Methods

The three methyl coumarates (Scheme 1) were synthesized according to a literature procedure.[14] The gas-phase absorption spectra were recorded at the electrostatic ion storage ring ELISA,[15] which has previously been used to study photoabsorption of biological chromophores (see, for example, reference [16]), and in particular those of the PYP.[9,10,17]

Briefly, deprotonated ions of the three PYP chromophore derivatives (shown in Scheme 1) were produced in the gas phase by using electrospray ionization. After pretrapping for up to 100 ms in a multipole ion trap with room temperature and having He as the buffer gas, a bunch of ions were accelerated to 22 keV, magnetically mass selected, and injected into ELISA. The chromophore ions were irradiated after storage for about 50 ms by a single laser-light pulse from an EKSPLA NT320 laser system with a tunable wavelength range from 210 to 2100 nm and a pulse duration of about 3 ns. In order not to damage the particle detector, we directed the laser beam transverse to the ion-beam direction in ELISA. This provided a smaller overlap region, but the signal was sufficiently strong that high quality data were readily obtained.

We used action spectroscopy to record the absorption spectrum of the chromophore ions. That is, the photoabsorption spectra were recorded by measuring the counts of neutral particles generated after laser excitation as a function of the wavelength. For the systems under study herein, the (electronic) excitation of the chromophore anions resulted in production of neutral photofragments within less than one revolution time in ELISA. Hence, the products were counted in a detector mounted right after the laser-excitation region (for details, see references [18] and [19]). The prompt photoaction may contain contributions from both fast fragmentation as well as electron emission. The advantage of using a storage ring, in which the target ions are stored at relatively high energies, is that although only neutral photofragments (and electrons) are created, a well-collimated beam of particles is available and detectable with high efficiency.

The ground-state geometries of the deprotonated *ortho*-, *meta*-, and *para*-methyl coumarates and their corresponding neutral radicals were optimized by using the functional B3LYP[20,21] along with the basis set aug-cc-pVDZ[22,23] as implemented in the program Gaussian 03.[24] Every stationary point of the potential energy surface was characterized as a local minimum by calculating the harmonic frequencies at the same level of theory. Adiabatic and vertical ionization potentials were obtained as differences of B3LYP/aug-cc-pVDZ energies. Vertical excitation energies were calculated with 1) the approximate coupled cluster singles and doubles CC2[25] linear response method in its efficient resolution of the identity variant[26,27] (RI-CC2), and 2) time-dependent DFT[28] using the functional

CAM-B3LYP[29] and the basis set aug-cc-pVTZ[22,23] in both cases. The auxiliary basis set used in the RI-CC2 calculations is that of Weigend et al.[30] The error concomitant with the RI approximation in the calculation of vertical excitation energies is expected to be negligible in comparison to the basis set error.[26] The effect of the *s-cis* and *s-trans* conformational isomerism on the excitation energies was addressed by the independent rotation of the angles ϕ_a and ϕ_b, as represented in Scheme 1 and a subsequent geometry optimization. Only 180° rotations were considered because rotating either ϕ_a or ϕ_b by a different amount would disrupt the planarity of the π system and reduce its extension: under these circumstances a blueshift would be expected.[16] The RI-CC2 and CAM-B3LYP approximations were used as implemented in the programs Turbomole 5.9.1[26,27,31,32] and Dalton 2.0,[33] respectively. The application of both methodologies with the basis set aug-cc-pVTZ has been shown to yield good results in the calculation of the electronic spectrum of the *p*CA$^-$ phenoxide anion.[10]

Results and Discussion

The gas-phase absorption spectra of *o*CMe$^-$, *m*CMe$^-$ and *p*CMe$^-$ are shown in Figure 1. It is noteworthy that our experimental technique allows us to record the absorption spectrum down to very short wavelength/high energy, and although some of the electronically excited states lie high in the continuum,[34] resonance states are nevertheless detectable.

It is observed that the *ortho* and *para* isomers have absorption maxima in the indigo region of the visible spectrum at 2.82 eV (439 nm) and 2.87 eV (432 nm), respectively, whereas *m*CMe$^-$ does not show a significant absorption around these energies. The disruption of the push–pull system in *m*CMe$^-$ produces a marked shift for the $S_0 \rightarrow S_1$ transition in comparison to the *ortho* and *para* isomers. As a consequence, the *meta* compound presents essentially no absorption in the energy span in which the photoactivity of the xanthopsins is observed ($\approx$2.67–2.86 eV). In fact, this chromophore has no absorptions in the wavelength interval between blue light and ultraviolet A. There are indications of a very weak absorption around 2.25 eV (550 nm), and our calculations (see below) support the presence of this band.

The absorption spectra of Figure 1 demonstrate that the push–pull system is critical for the wavelength associated with the $S_0 \rightarrow S_1$ transition of *p*CA$^-$, which triggers the photoactivity of the xanthopsins. Moreover, a comparison of the spectra in Figure 1 reveals that the naturally occuring *p*CA$^-$ is the positional isomer that absorbs most strongly in the indigo region of the visible spectrum. This is relevant for the biological action of these proteins in view of their low abundance in the cytoplasm: *H. halophila* has only around of 500 PYP molecules per cell.[2]

The chromophores *o*CMe$^-$ and *m*CMe$^-$ absorb strongly in the UV: the most intense absorption band of the *meta*

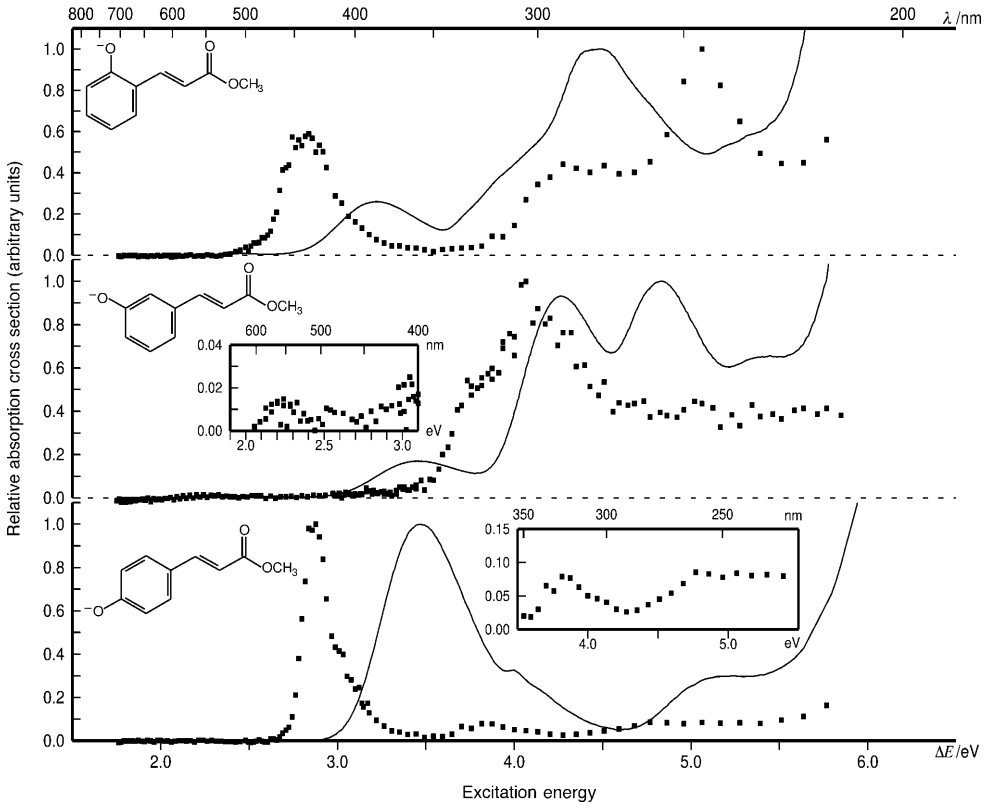

Figure 1. Photoabsorption spectra of the deprotonated *ortho*-, *meta*-, and *para*-methyl coumarates in the gas phase (■) and in methanol (——). Every spectra is normalized to one at maximum absorption. The phenoxides in methanol have Na^+ as the counterion. The solution of *o*CMe$^-$Na$^+$ also contains δ-lactone formed from intramolecular cyclization.

isomer is at 4.11 eV (302 nm) with a shoulder at 3.75 eV (331 nm), whereas the *ortho* compound has strong absorptions at 4.28 eV (290 nm) and 5.06 eV (245 nm). The chromophore model pCMe$^-$ also presents maxima of absorption in the UV at 3.84 eV (323 nm) and 4.77 eV (260 nm), but these bands are considerably less intense than the $S_0 \rightarrow S_1$ excitation.

The absorption spectra of the three chromophores in methanol are also shown in Figure 1. The lowest-energy absorption maxima of oCMe$^-$, mCMe$^-$, and pCMe$^-$ in methanol are at 3.25 eV (382 nm), 3.48 eV (356 nm) and 3.48 eV (356 nm), respectively. Thus, solvation by methanol results in significant hypsochromism for all three chromophores. The shifts in methanol suggest a significant change in the electric dipole moment, $|\Delta\boldsymbol{\mu}|$, in the $S_0 \rightarrow S_1$ excitation of the three chromophores, as confirmed by our calculations. The lowest-energy absorptions are similar in methanol: in particular, for the *meta* and *para* chromophores, but with significant differences in the oscillator strengths. It is noteworthy that the solution of oCMe$^-$ in methanol contains the lactone resulting from intramolecular cyclization. This impurity is avoided in the gas-phase experiments with mass-selected ionic chromophores.

The theoretical gas-phase absorption spectra at the RI-CC2/aug-cc-pVTZ and CAM-B3LYP/aug-cc-pVTZ levels of theory are shown in Figure 2. There is good overall agreement between theory and experiment. The RI-CC2/aug-cc-pVTZ $S_0 \rightarrow S_1$ vertical excitations of oCMe$^-$ and pCMe$^-$ are located in the high-energy region of the visible spectrum at 2.64 eV (470 nm) and 3.10 eV (400 nm), respectively, in good accordance with experiment. The magnitude of the calculated oscillator strengths are 0.417 (oCMe$^-$) and 1.044 (pCMe$^-$). Regarding the *meta* isomer, the $S_0 \rightarrow S_1$ vertical excitation is predicted to be at 2.27 eV (546 nm) at the RI-CC2/aug-cc-pVTZ approximation. This excitation has a small oscillator strength ($\approx 10^{-2}$), substantiating the weak absorption signal observed at 2.25 eV in the gas-phase spectra of mCMe$^-$. All calculated vertical excitations from the low-wavelength part of the visible spectrum (blue and violet light) to the near UV of the *meta* isomer have oscillator strengths in the order of 10^{-3}, in correspondence with the absence of strong experimental bands in this wavelength range (see Figure 1). There is also a good correlation between theory and experiment with respect to the absorption of the three chromophores in the UV region. For mCMe$^-$, for example, the states corresponding to the most intense absorption peak, and the corresponding shoulder, are predicted to be at 4.34 eV (286 nm) and 4.16 eV (298 nm), respectively, while the experimental values are 4.11 eV (302 nm) and 3.85 eV (322 nm), respectively.

The presence of *s-cis* and *s-trans* conformers could significantly affect the absorptions for oCMe$^-$, mCMe$^-$, and pCMe$^-$. We therefore investigated the effect of the rotation of the dihedral angles ϕ_a and ϕ_b (see Scheme 1) on the verti-

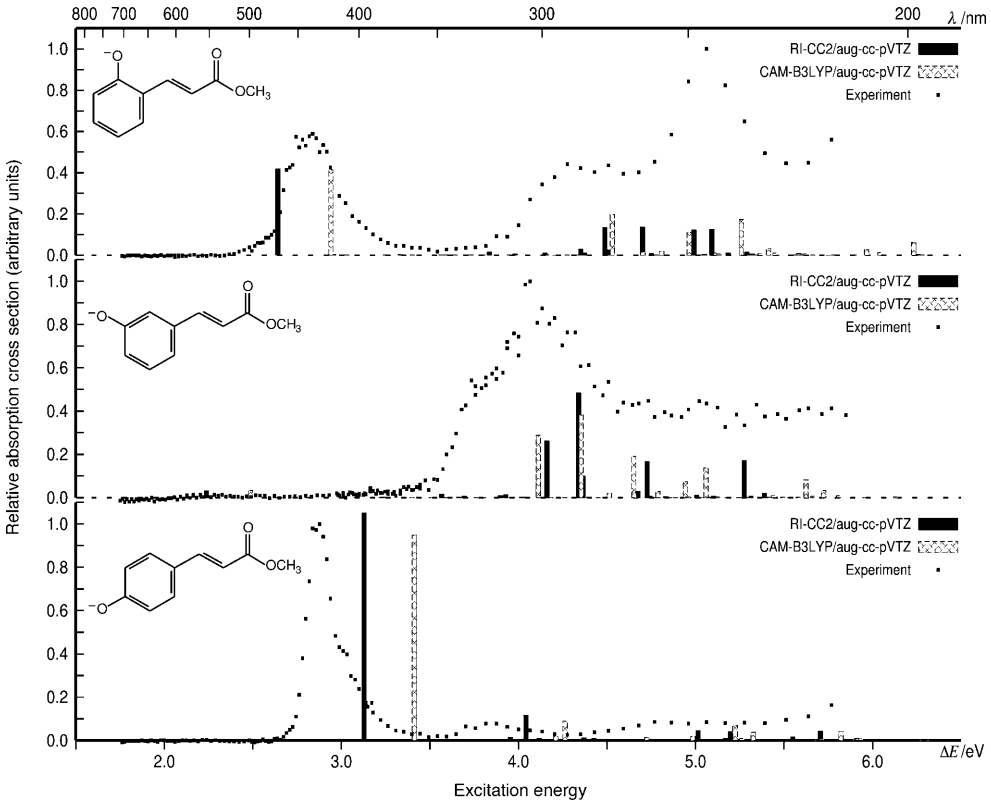

Figure 2. Gas-phase absorption spectra of the deprotonated *ortho*-, *meta*- and *para*-methyl coumarates calculated at the RI-CC2/aug-cc-pVTZ and CAM-B3LYP/aug-cc-pVTZ levels of theory. The experimental spectra are presented for comparison.

cal excitations of the considered conformers.[35] The rotation around the bond between the carbonyl and the α carbon (i.e., a change in ϕ_a) has almost no effect on the calculated vertical excitations of the three isomers, whereas the gyration around the bond linking the β and γ carbon atoms[36] (i.e., a modification in ϕ_b) in *o*CMe$^-$ and *m*CMe$^-$ has more appreciable effects on the calculated spectra. For instance, the RI-CC2/aug-cc-pVTZ absorption spectra of the conformers of *m*CMe$^-$ with the phenoxy oxygen in an *s-trans* position with respect to the β hydrogen ($\phi_b = 0.0$) have their most intense absorption at 4.34 and 4.37 eV, whereas for the *s-cis* conformers ($\phi_b = 180.0$) the bright state is less dominating. Similar effects can be described in the UV for *o*CMe$^-$. Another important effect of the conformational equilibrium of *o*CMe$^-$ is on the $S_0 \rightarrow S_1$ vertical excitation, which changes noticeably as a function of the dihedral ϕ_b: those conformers with $\phi_b = 0.0$ have RI-CC2/aug-cc-pVTZ vertical excitation energies of 2.64 eV (470 nm) and 2.67 eV (464 nm), while the corresponding values of the systems with $\phi_b = 180.0$ are 2.94 eV (422 nm) and 2.95 eV (420 nm). The peak broadening in the experimental absorption of the $S_0 \rightarrow S_1$ transition can be related to this dependence of the vertical excitation energies on the dihedral angle ϕ_b, in virtue that the four conformers of *o*CMe$^-$ are nearly isoenergetic.[37] Thus, the four conformers may be present in significant amounts when the spectrum is recorded. It should of course be noted that the shape of a band for a particular configuration is determined by the form of the excited-state potential energy surface. Thus, a steep repulsive Franck–Condon region of the excited state can cause significant broadening of a band.[38,39]

The description of the absorption spectra by the approximation CAM-B3LYP/aug-cc-pVTZ is analogous to that offered by the RI-CC2/aug-cc-pVTZ level of theory. There is a systematic small blueshift for the absorptions predicted by CAM-B3LYP with respect to those obtained using RI-CC2, but the description is similar enough to encourage the application of CAM-B3LYP in theoretical studies addressing larger models of PYP.

The conjugation between the electron-withdrawing group $-COOCH_3$ and the electron-donating phenoxy oxygen, which causes the pronounced differences in the absorption spectra of the *meta* isomer in comparison with the *ortho* and *para* anions, can be analyzed in terms of the bond lengths along the π system, as shown in Figure 3. The three chromophores present a similar −C–O$^-$ bond length in the phenoxy ring, which is considerably shorter than the C–O bond length in phenol (1.37 Å[40]). The bonds between the *ipso*- (with respect to the group −O$^-$) and the *ortho*-carbon atoms are the longest in the aromatic ring for the three isomers, indicating that there is a substantial delocalization of the negative charge in the aromatic ring, as shown in Scheme 2 for *m*CMe$^-$. The largest difference in the bond lengths of the π system between the *meta* isomer and its *ortho* and *para* analogues is for the bond between the β and γ carbon atoms: this bond is 0.04 (0.03) Å larger in *m*CMe$^-$ than in *p*CMe$^-$ (*o*CMe$^-$). This bond links the electron-donor group to the

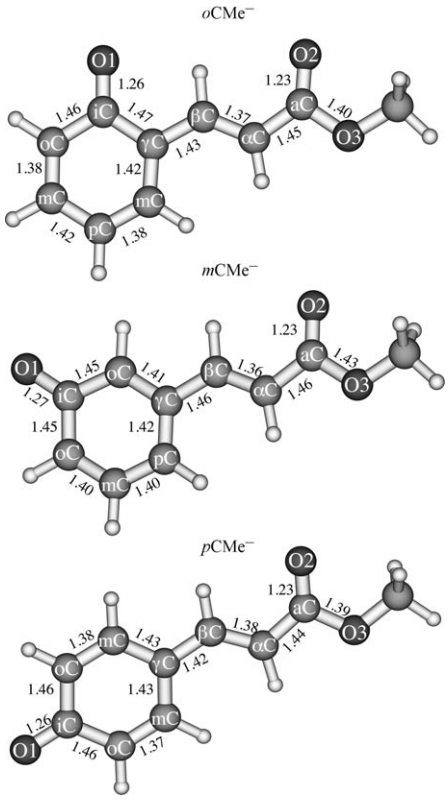

Figure 3. Bond lengths in Å throughout the π systems of the deprotonated *ortho*-, *meta*- and *para*-methyl coumarates. The labels iC, oC, mC, pC denote the *ipso*-, *ortho*-, *meta*-, and *para*-carbon atoms, respectively, with reference to the phenoxy oxygen, while aC, αC, βC, and γC indicate the acyl, alpha, beta, and gamma carbon atoms of the unsaturated ester.

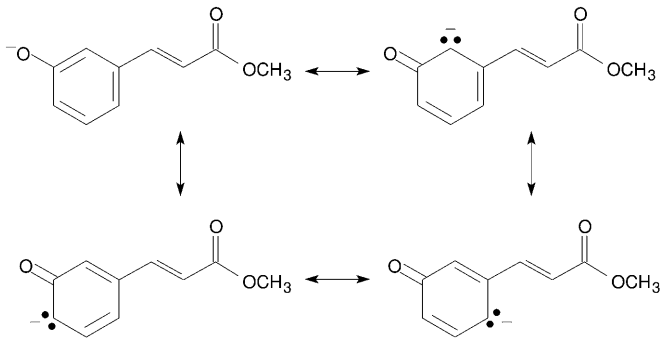

Scheme 2. Delocalization of the negative charge on the oxygen atom in the aromatic ring of the deprotonated *m*-methyl coumarate. The *ortho* and *para* analogues exhibit a similar delocalization.

electron-withdrawing α,β-unsaturated carbonyl. Similarly, the bond joining the α and the acyl carbon atoms (i.e., connecting the −C=C− moiety and the electron-withdrawing group $-COOCH_3$) is shorter in *p*CMe$^-$ and *o*CMe$^-$. This suggests that the delocalization of the negative charge of the phenoxy oxygen in the *ortho* and *para* anions is further increased by the $-COOCH_3$ group with respect to the *meta* isomer, leading to different $S_0 \rightarrow S_1$ excitation energies.

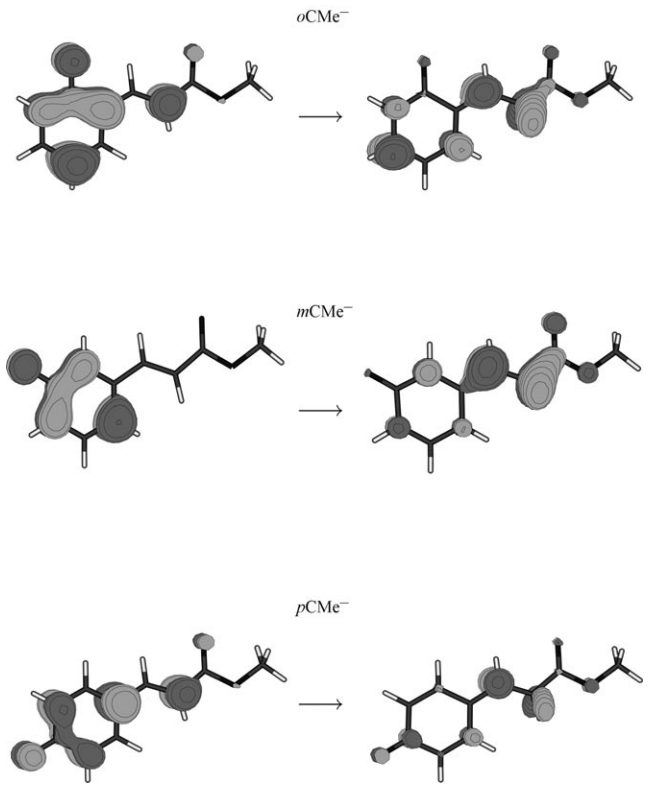

Figure 4. Molecular orbitals involved in the principal components of the $S_0 \rightarrow S_1$ transition for *o*CMe$^-$, *m*CMe$^-$, and *p*CMe$^-$.

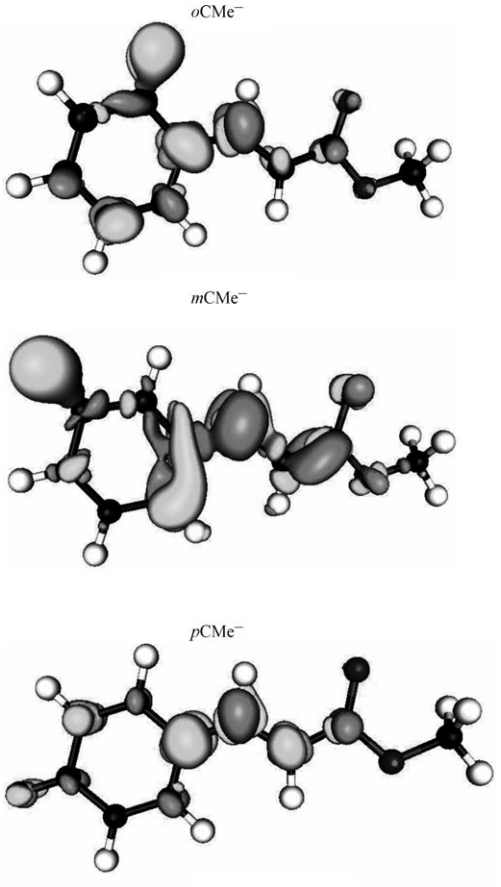

Figure 5. Differential RI-CC2/aug-cc-pVTZ electron density for the transition $S_0 \rightarrow S_1$ of the deprotonated *ortho*-, *meta*-, and *para*-methyl coumarates. The dark and light gray surface levels represent negative and positive values, respectively, of the differential electron density.

The $S_0 \rightarrow S_1$ transitions in the three isomers are dominated by $\pi \rightarrow \pi^*$ transitions. The involved orbitals are shown in Figure 4. The HOMO of *m*CMe$^-$ does not extend to the α,β-unsaturated carbonyl as in *o*CMe$^-$ and *p*CMe$^-$, reflecting a smaller degree of electron delocalization in *m*CMe$^-$ and a more hindered push–pull system. The most intense transition of the *m*CMe$^-$ has $\pi \rightarrow \pi^*$ transitions as its major components as well. Regarding the intensity of the predicted bands, the A'' states, which are composed of excitations involving orbitals with different symmetries, have negligible oscillator strengths. As seen in Figure 5, the character of the $S_0 \rightarrow S_1$ transition is similar for the three chromophores with a charge transfer from the phenoxy ring to the acylic moiety of the chromophore. The charge-transfer character is considerably larger for the *meta* isomer: the magnitude of the change in dipole moment associated with the $S_0 \rightarrow S_1$ excitation is 2.81, 10.39, 2.97 D for the *ortho*-, *meta*-, and *para*-methyl coumarates, respectively. This suggests a larger solvatochromic effect for this transition of the *meta* isomer as indeed seen in the spectra given in Figure 1.

The blueshift caused by methanol may be rationalized by considering the flow of charge depicted in Figure 5. The stronger hydrogen bonds are those formed between hydrogen-donating methanol molecules and the negatively charged $-C_6H_4-O^-$. In this way, the phenoxy oxygen donates electron density to the hydrogen-bond donors, impairing the charge transfer to the carbonyl, and hence, inducing the observed blueshift. The attachment of two water molecules to the phenolic moiety of *p*CA$^-$[17,41] and the amino acids Glu46 and Tyr42 within the protein lead to a hypsochromic effect[42,43] for the same reason. It is noteworthy, however, that the blueshift caused by Glu46 and Tyr42 is considerably smaller than that observed in alcohol solutions, implying a larger effect on the relative energies of the different electronic states by the solvation shell, as discussed in reference [9]. The substantial change in dipole moment for *o*CMe$^-$, *m*CMe$^-$, and *p*CMe$^-$ is in agreement with the strong solvatochromism observed in Figure 1 and it indicates that the excitation energies are particularly susceptible to the nature of the environment.

Conclusion

The gas-phase absorption spectra of the *trans ortho*-, *meta*-, and *para*-methyl coumarates were measured in an effort to assess the relevance of the push–pull system in the absorption of the *trans p*-coumaric acid, the chromophore within the PYP and other xanthopsins. The systems with the electron-donating phenoxy and the electron-withdrawing acyl groups in conjugation, that is, the *ortho*- and *para*-methyl

coumarates, have the $S_0 \rightarrow S_1$ transition in the wavelength interval where the activity of the xanthopsins is observed, whereas the corresponding excitation for the *meta* isomer is strongly shifted and weakened. The *meta* compound has no absorption in the wavelength range from ultraviolet A to blue light, while its most intense absorption is observed in the limits between the near and middle ultraviolet. This demonstrates the importance of the push–pull system in the absorption of *trans p*-coumaric acid. In addition, *trans p*-methyl coumarate is the chromophore model that absorbs most intensely in the indigo region, and hence, it represents the most suitable substitution pattern (*ortho*-, *meta*-, *para*-) for the biological action of the xanthopsins. The linear response calculations at the RI-CC2/aug-cc-pVTZ and CAM-B3LYP/aug-cc-pVTZ levels of theory agree, in general, with experiments in the description of the absorption spectra of the methyl coumarates and give support to the very weak absorption of the *meta* isomer around 2.25 eV (550 nm) presumably associated with the $S_0 \rightarrow S_1$ transition. The *meta* isomer has a weaker coupling between donor and acceptor ends, that is, the HOMO and LUMO are separately located at each end of the molecule, which means that the transition has a higher degree of charge transfer for this regioisomer. Solvation effects mask this important finding when comparing the absorption spectra in solution. The differential density plots gave insights on the hypsochromic effect of methanol and provide a basis to rationalize the blueshift caused by the hydrogen bonds of Glu46 and Tyr42 to the phenoxy moiety of the chromophore within the protein.

Acknowledgements

This work was supported by the Lundbeck Foundation, Carlsberg Foundation and Willum Kann Rasmussen Foundation, and the Danish Research Agency (Contract No. 272-06-0427). O.C. also gratefully acknowledge support from the Danish Center for Scientific Computing (DCSC), the Danish National Research Foundation and EUROHORCs for a EURYI award.

[1] J. Hendriks, K. J. Hellingwerf, *Photoactive Yellow Protein: The Prototype Xanthopsin in Handbook of Organic Photochemistry and PhotoBiology* (Eds.: W. Horspool, F. Lenci), CRC Press, New, **2004**, pp. 123/1–22.
[2] D. S. Larsen, R. van Grondelle, K. J. Hellingwerf, *Primary Photochemistry in the Photoactive Yellow Protein: The PRototype Xanthopsin in Ultrashort Laser Pulses in Biology and Medicine* (Eds.: M. Braun, P. Gilch, W. Zinth), Springer, ,Heidelberg, . **2007**, pp. 165–199.
[3] M. A. van der Horst, K. J. Hellingwerf, *Acc. Chem. Res.* **2004**, *37*, 13–20.
[4] W. W. Sprenger, W. D. Hoff, J. P. Armitage, K. J. Hellingwerf, *J. Bacteriol.* **1993**, *175*, 3096–3104.
[5] Z.-Y. Jiang, L. R. Swem, B. G. Rushing, S. Devanathan, G. Tollin, C. E. Bauer, *Science* **1999**, *285*, 406–409.
[6] K. J. Hellingwerf, J. Hendriks, T. Gensch, *J. Phys. Chem. A* **2003**, *107*, 1082–1094.
[7] R. R. Birge, *Annu. Rev. Phys. Chem.* **1990**, *41*, 683–733.
[8] L. H. Andersen, I. B. Nielsen, M. B. Kristensen, M. O. A. El Ghazali, S. Haacke, M. Brøndsted Nielsen, M. Å. Petersen, *J. Am. Chem. Soc.* **2005**, *127*, 12347–12350.
[9] I. B. Nielsen, S. Boyé-Péronne, M. O. A. El Ghazaly, M. B. Kristensen, S. B. Nielsen, L. H. Andersen, *Biophys. J.* **2005**, *89*, 2597–2604.
[10] T. Rocha-Rinza, O. Christiansen, J. Rajput, G. Aravind, D. B. Rahbek, L. H. Andersen, A. V. Bochenkova, A. A. Granovsky, K. B. Bravaya, A. V. Nemukhin, K. L. Christiansen, M. B. Nielsen, *J. Phys. Chem. A* **2009**, *113*, 9442–9449.
[11] For the xanthopsin in *Thermochromatium tepidum* studied in reference [12].
[12] J. A. Kyndt, J. C. Fitch, T. E. Meyer, M. A. Cusanovich, *Biochemistry* **2005**, *44*, 4755–4764.
[13] For the xanthopsin in *Rhodospirillum centenum* studied in reference [5].
[14] S. Karthikeyan, V. Ramamurthy, *J. Org. Chem.* **2007**, *72*, 452–458.
[15] S. P. Møller, *Nucl. Instrum. Methods Phys. Res. Sect. A* **1997**, *394*, 281–286.
[16] L. H. Andersen, A. V. Bochenkova, *Eur. Phys. J. D* **2009**, *51*, 5–14.
[17] J. Rajput, D. B. Rahbek, G. Aravind, L. H. Andersen, *Biophys. J.* **2010**, *98*, 488–492.
[18] L. H. Andersen, A. Lapierre, S. B. Nielsen, I. B. Nielsen, S. U. Pedersen, U. V. Pedersen, S. Tomita, *Eur. Phys. J. D* **2002**, *20*, 597–600.
[19] L. Lammich, J. Rajput, L. H. Andersen, *Phys. Rev. E* **2008**, *78*, 051916–1:051916–6.
[20] A. D. Becke, *J. Chem. Phys.* **1993**, *98*, 5648–5652.
[21] P. J. Stephens, F. J. Devlin, C. F. Chabalowski, M. J. Frisch, *J. Phys. Chem.* **1994**, *98*, 11623–11627.
[22] T. H. Dunning, *J. Chem. Phys.* **1989**, *90*, 1007–1023.
[23] R. A. Kendall, T. H. Dunning, R. J. Harrison, *J. Chem. Phys.* **1992**, *96*, 6796–6806.
[24] Gaussian 03, Revision D.01, M. J. Frisch, G. W. Trucks, H. B. Schlegel, G. E. Scuseria, M. A. Robb, J. R. Cheeseman, Montgomery, Jr., J. A., T. Vreven, K. N. Kudin, J. C. Burant, J. M. Millam, S. S. Iyengar, J. Tomasi, V. Barone, B. Mennucci, M. Cossi, G. Scalmani, N. Rega, G. A. Petersson, H. Nakatsuji, M. Hada, M. Ehara, K. Toyota, R. Fukuda, J. Hasegawa, M. Ishida, T. Nakajima, Y. Honda, O. Kitao, H. Nakai, M. Klene, X. Li, J. E. Knox, H. P. Hratchian, J. B. Cross, V. Bakken, C. Adamo, J. Jaramillo, R. Gomperts, R. E. Stratmann, O. Yazyev, A. J. Austin, R. Cammi, C. Pomelli, J. W. Ochterski, P. Y. Ayala, K. Morokuma, G. A. Voth, P. Salvador, J. J. Dannenberg, V. G. Zakrzewski, S. Dapprich, A. D. Daniels, M. C. Strain, O. Farkas, D. K. Malick, A. D. Rabuck, K. Raghavachari, J. B. Foresman, J. V. Ortiz, Q. Cui, A. G. Baboul, S. Clifford, J. Cioslowski, B. B. Stefanov, G. Liu, A. Liashenko, P. Piskorz, I. Komaromi, R. L. Martin, D. J. Fox, T. Keith, M. A. Al-Laham, C. Y. Peng, A. Nanayakkara, M. Challacombe, P. M. W. Gill, B. Johnson, W. Chen, M. W. Wong, C. Gonzalez, J. A. Pople, Gaussian, Inc., Wallingford, CT, **2004**.
[25] O. Christiansen, H. Koch, P. Jørgensen, *Chem. Phys. Lett.* **1995**, *243*, 409–418.
[26] C. Hättig, F. Weigend, *J. Chem. Phys.* **2000**, *113*, 5154–5161.
[27] C. Hättig, A. Köhn, *J. Chem. Phys.* **2002**, *117*, 6939–6951.
[28] M. A. L. Marques, E. K. U. Gross, *Annu. Rev. Phys. Chem.* **2004**, *55*, 427–455.
[29] T. Yanai, D. P. Tew, N. C. Handy, *Chem. Phys. Lett.* **2004**, *393*, 51–57.
[30] F. Weigend, A. Köhn, C. Hättig, *J. Chem. Phys.* **2002**, *116*, 3175–3183.
[31] O. Treutler, R. Ahlrichs, *J. Chem. Phys.* **1995**, *102*, 346–354.
[32] M. von Arnim, R. Ahlrichs, *J. Comput. Chem.* **1998**, *19*, 1746–1757.
[33] DALTON, a molecular electronic structure program, Release 2.0, **2005**, see: http://www.kjemi.uio.no/software/dalton/dalton.html.
[34] The vertical ionization potentials of *o*-CMe^-,*m*-CMe^- and *p*-CMe^- are 2.90, 2.75, and 3.01 eV, respectively, while the corresponding adiabatic values are (in the same order) 2.82, 2.67, and 2.92 eV.
[35] The vertical excitations and the calculated spectra of all the studied conformers can be found in the Supporting Information.
[36] The nomenclature of the atoms is shown in Figure 4.
[37] The difference between the most stable and the less stable conformer of $oCMe^-$ at the B3LYP/aug-cc-pVDZ//RI-CC2/aug-cc-pVTZ level is less than 2 kcal mol^{-1}.

[38] This effect is known as the reflection principle and it is described in reference [39].
[39] R. Schinke, *Photodissociation Dynamics: Spectroscopy and Fragmentation of Small Polyatomic Molecules.* Cambridge University Press, New York, **1995**.
[40] C. Ratzer, J. Küpper, D. Spangenberg, M. Schmitt, *Chem. Phys.* **2002**, *283*, 153–169.
[41] E. V. Gromov, I. Burghardt, J. T. Hynes, H. Köppel, L. S. Cederbaum, *J. Photochem. Photobiol. A* **2007**, *190*, 241–257.
[42] S. Devanathan, R. Brudler, B. Hessling, T. T. Woo, K. Gerwert, E. D. Getzoff, M. A. Cusanovich, G. Tollin, *Biochemistry* **1999**, *38*, 13766–13772.
[43] E. V. Gromov, I. Burghardt, H. Köppel, L. S. Cederbaum, *J. Am. Chem. Soc.* **2007**, *129*, 6798–6806.

Received: February 16, 2010
Revised: May 26, 2010
Published online: September 8, 2010

